IJC Heart & Vasculature 39 (2022) 101004

Contents lists available at ScienceDirect

IJC Heart & Vasculature

journal homepage: www.sciencedirect.com/journal/ijc-heart-and-vasculature

# Three simple but interesting transthoracic echocardiographic road maps for proximal superior vena cava visualisation in healthy young adults

Mohammadbagher Sharifkazemi *, Gholamreza Rezaian, Elham Hosseininejad, Alireza Arjangzadeh

*Department of Cardiology, Nemazee Hospital, Shiraz University of Medical Sciences, Shiraz, Iran*

ARTICLE INFO

*Keywords:*
Superior Vena Cava
Transthoracic visualization
Modified transthoracic views
Two-dimensional echocardiography

ABSTRACT

*Background:* Although much is known about the technical aspects of inferior vena cava visualization, it is much less about its counterpart: the superior vena cava (SVC). The aims of this study therefore, were to describe in detail the different possible two dimensional echocardiographic SVC visualization techniques in healthy young adults and to provide a series of values for its dimensions and Doppler signals.

*Methods:* The proximal SVC visualization through the three transthoracic windows was initially established in several adult patients, with or without cardiovascular implantable devices. Subsequently a group of 70 completely healthy adults (35 males and 35 females) were studied to determine the values of SVC dimensions and its pulse Doppler signal characteristics. The visualization windows included: a) Modified apical 5-champber view, b) Modified parasternal short axis view of great vessels and c) Modified subcostal view. The SVC dimensions were measured 3–5 cm above the RA-SVC junction at the end of both hold cardiac and respiratory cycles (systole, diastole and inspiration/expiration, respectively). The peak pulse Doppler velocities were only measured at the end-held expiration.

*Results:* The largest end systolic proximal SVC dimensions at the end of the expiration and inspiration ranged from 8 to 14.0 mm (11 ± 2 mm) and 8.0–14.0 mm (11 ± 2 mm) respectively, and the highest S wave velocity ranged from 0.5 to 0.7 m/s (0.6 ± 0.0 m/s).

*Conclusion:* This study has provided a detailed technical description for transthoracic proximal SVC visualization in a group of 70 healthy adults and has furnished sets of values for its dimensions and Doppler signal parameters.

## 1. Introduction

The superior vena cava (SVC) is formed by the right and left brachiocephalic (innominate) veins and receives the venous return from the upper part of the body above the diaphragm. It then passes vertically downwards and after receiving the azygous vein it joins the upper and posterior part of the right atrium at the level of the third costal cartilage [1].

The right supraclavicular and less frequently suprasternal windows for SVC visualization have been in use for many years, but until recently the true conventional transthoracic ones were ignored, partly because of the presence of poor acoustic windows. In the most recent echocardiographic guidelines, however, the possibility of seeing SVC through most of these transthoracic windows has been brought about [2], but what actually is missing, is the technical description and details of how to do it, which in addition to other reasons, has made SVC imaging to be neglected as a standard part of routine transthoracic echocardiographic evaluation.

The SVC is the largest central systemic vein in the mediastinum and like other important constituents of cardiovascular system, can be affected by a wide variety of congenital and acquired abnormalities totally independent from those of the IVC.

Persistent left SVC, partial anomalous pulmonary venous drainage and SVC aneurysm are some of the congenital abnormalities which are mainly asymptomatic and may be detected incidentally in subjects undergoing imaging for cardiac or other indication.

In addition, acquired abnormalities such as primary neoplasms, trauma, fibrin sheath, intrinsic or extrinsic strictures can produce mild

*Abbreviations:* SVC, Superior vena cava; TTE, Transthoracic echocardiography; MA5CV, Modified apical 5-chamber view; MSAVGV, Modified parasternal short axis view of great vessels; MSCV, Modified subcostal view.

* Corresponding author at: Department of Cardiology, Nemazee Hospital, Nemazee Square, Shiraz 71846141478, Iran.
*E-mail address:* dr.sharifkazemi@gmail.com (M. Sharifkazemi).

https://doi.org/10.1016/j.ijcha.2022.101004
Received 8 December 2021; Received in revised form 20 February 2022; Accepted 9 March 2022

compression or total occlusion, the so called SVC syndrome.

SVC occlusion is an important clinical entity that requires urgent diagnosis and treatment. It may be caused by extravascular compression or intravascular thrombosis, mediastinal masses [3], central venous catheters [4], pacemaker wires [5,6] and radiofrequency ablation for ectopic atrial tachycardia are only some of the many causes of SVC obstruction [7]. Satisfactory visualization of SVC, therefore, could be quite helpful for proper diagnosis and selection of appropriate treatment. The aim of our study therefore is to report the fine technical details for SVC visualization through the conventional transthoracic as well as subcostal echocardiographic windows and some of its parameters in a group of young adults free of cardiopulmonary disease, hypertension and obesity.

## 2. Methods

### 2.1. Subjects

#### 2.1.1. Inclusion Criteria:

Subjects were included in the study only if they fulfilled all the following criteria: a) being young, completely healthy and having no underlying illness or cardiovascular risk factor including obesity. b) having normal general physical examination including the cardiovascular system. c) having a completely normal electrocardiogram and conventional 2DE and d) having proper windows for all the three conventional parasternal, apical and subcostal echocardiographic views. After documenting the feasibility of proximal SVC visualization by the three conventional transthoracic echocardiographic views, the technique was applied in a group of 151 young healthy adult volunteers of whom 70, including 35 males and 35 females fulfilled the inclusion criteria and were enrolled for the final assessment.

The remaining fifty-one participants had only one or two proper windows, thus were excluded. However, proximal SVC visualization was possible through at least one window in all participants.

All participants signed a written consent and the study protocol was approved by the local ethics committee.

### 2.2. Techniques

#### 2.2.1. Road 1: The Modified apical 5-Chamber view (MA5CV)

The subjects were positioned half-way between supine and left lateral decubitus. Then the transducer was placed in the 5th intercostal space at the anterior axillary line with the index mark pointing to the patient's right shoulder to obtain an apical 5-chamber view. By gentle side tilting the transducer more medially (between −40 to −80 degrees), the proximal SVC could be visualized and studied (Fig. 1A).

#### 2.2.2. Road 2: The Modified parasternal short axis view of great vessels (MSAVGV)

The participants were slightly turned to the left, somewhere between supine and left lateral decubitus position. Then the transducer was put in the 3rd intercostal space, close to the sternal border with the index mark pointing to the suprasternal notch. By mild and gentle tilting of the transducer toward the right shoulder (between −15 to −30 degrees) the proximal SVC could be seen and assessed in this view (Fig. 1B).

#### 2.2.3. Road 3: The Modified subcostal view (MSCV)

The subjects were put in supine position and were asked to flex the knees to relax the abdominal wall muscles. Then the transducer was positioned a bit lateral to the upper mid-epigastric region, with the index mark pointing to the mid-right clavicular area. By tilting the probe toward the right shoulder (between −15 to −45 degrees depending on the subject's cardiac position), the proximal SVC was visualized (Fig. 1C).

### 2.3. Measurement of proximal SVC dimensions and Doppler parameters

The proximal SVC dimensions were measured 3–5 mm proximal (above) the RA-SVC junction, both at the end of systole and diastole, and deep held inspiration and expiration. The pulse Doppler measurement, however, was performed only at the end of held expiration, color guided, proximal (above) the RA-SVC junction and using a 3 mm sample volume size. In addition, to clarify the SVC color flow, the Nyquist limit was set at 25 to 40 cm/sec (Fig. 2A-C, 3A-C & 4A-C). In addition, the SVC course with final right atrial (RA) filling was clarified through left-brachial vein injection of agitated saline (Fig. 4D).

### 2.4. Statistical methods

Data are expressed as mean ± SD. All numbers are rounded to a maximum of one decimal. However, no decimals were used for measurements given in millimetre.

Intraclass correlation coefficient was measured to assess the reproducibility of the study data and a p-value $\leq 0.05$ was considered significant.

### 2.5. Ethics declarations

The study protocol was approved by the Institutional Ethics Committee of Shiraz University of Medical Sciences (Code: IR.SUMS.MED.REC.1398.366). All procedures performed in this study were in accordance with the ethical standards of the institutional and/or national research committee and with the 1964 Helsinki declaration and its later amendments. All the participants signed a written informed consent.

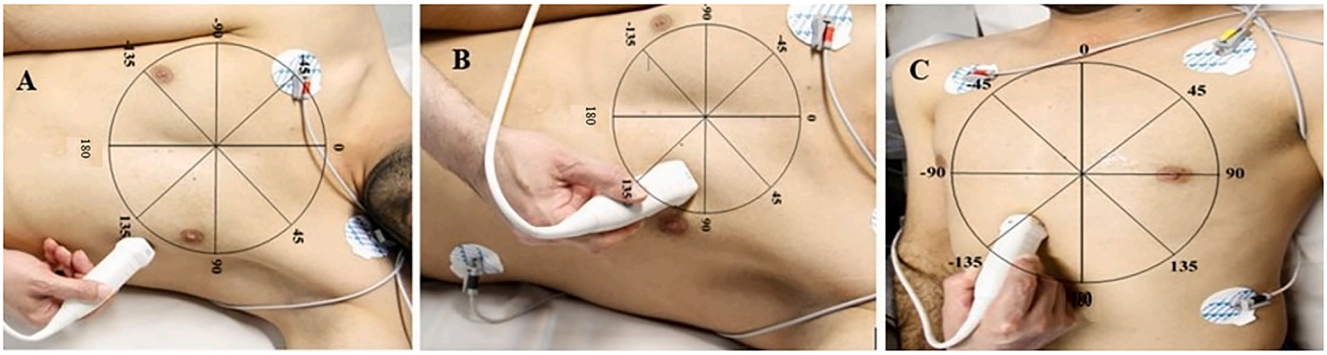


**Fig. 1.** Proximal SVC visualization through the three conventional transthoracic two dimensional echocardiographic windows. **A**) Patient in left lateral decubitus position for taking modified apical five chamber view. **B)** Patient mildly turned to the left between supine and left lateral position for taking the modified parasternal short axis view of great vessels. **C)** Patient in supine position for taking the modified subcostal view.

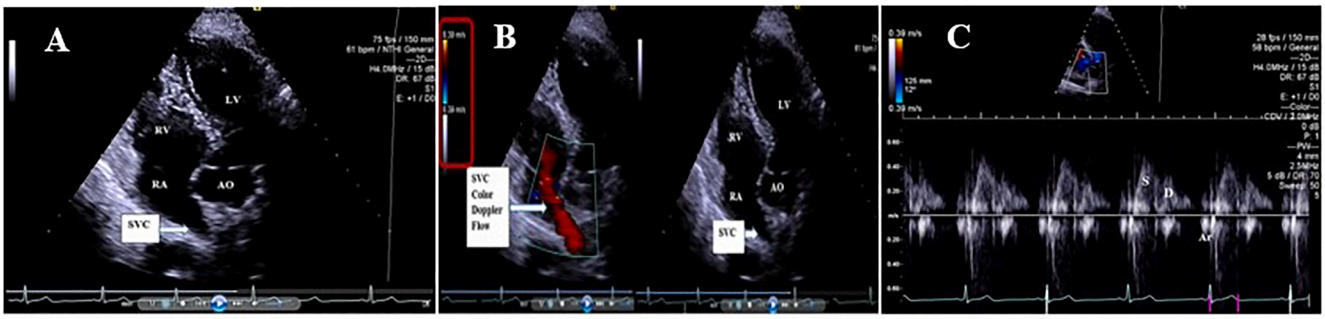


**Fig. 2.** Modified apical five chamber view. **A)** Two dimensional modified apical five chamber view for demonstration of proximal SVC. **B)** SVC Color Doppler flow (red in color; flow towards the probe) from modified apical five chamber view. Simultaneous 2D and Color Doppler Images. **C)** SVC Pulse Wave Doppler from modified apical five chamber view. SVC, superior vena cava; RA, right atrium; RV, right ventricle; AO, aorta; LV, left ventricle; S, systolic forward flow; D, diastolic forward flow; Ar, atrial flow reversal. (For interpretation of the references to color in this figure legend, the reader is referred to the web version of this article.)

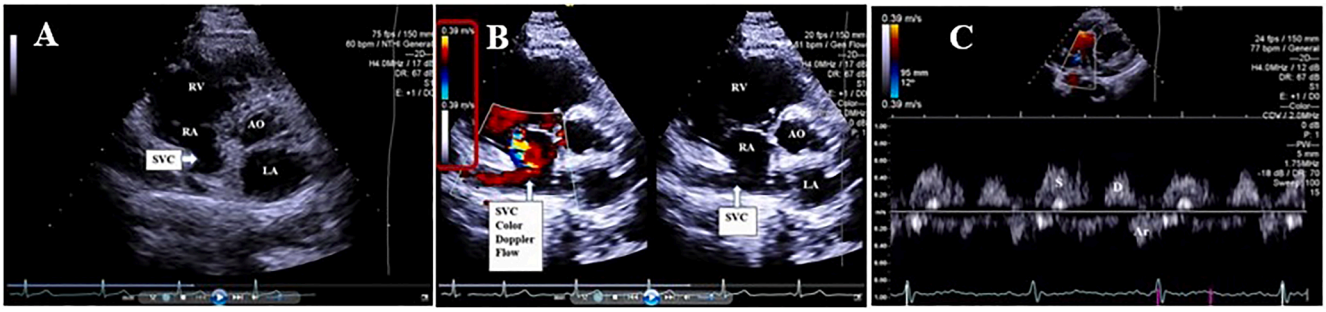


**Fig. 3.** Modified parasternal short axis view of great vessels. **A)** Two dimensional modified parasternal short axis view of great vessels for proximal SVC visualization. **B)** SVC Color Doppler flow (red in color; flow towards the probe) from modified parasternal short axis view of great vessels. Simultaneous 2D and Color Doppler Images. **C)** SVC Pulse Wave Doppler from modified parasternal short axis view of great vessels. SVC, superior vena cava; RA, right atrium; RV, right ventricle; AO, aorta; LA, left atrium; S, systolic forward flow; D, diastolic forward flow; Ar, atrial flow reversal. (For interpretation of the references to color in this figure legend, the reader is referred to the web version of this article.)

## 3. Results

The demographic data of the studied subjects are shown in Table 1 and the proximal SVC dimensions and the Doppler parameters are shown in tables 2 and 3 respectively. The intraclass correlation coefficients of proximal SVC dimensions and velocities are presented in tables 4 and 5.

Pulse wave Doppler interrogation of proximal SVC revealed three distinct wave forms. The largest of the three wave forms is the S-wave, which occurs during right ventricular systole and is formed by the rush of blood from the SVC into the RA. The second wave form, the D-wave, occurs during early diastole when tricuspid valve opens and rapid ventricular filling happens and finally RA contraction results in a brief flow reversal leading to the development of the third wave (Ar wave) (Fig. 2C, 3C & 4C) (Video image).

## 4. Discussion

This study has provided detailed technical description for transthoracic proximal SVC visualization in adults, through the three conventional transthoracic echocardiographic windows. It has also furnished a series of transthoracically obtained values for proximal SVC dimensions and their respiratory variations as well as its Doppler velocity signals.

SVC visualization and its parameters can provide useful information helping the bedside diagnosis of certain cardiac and non-cardiac disorders. In majority of normal subjects, inspiration increases the magnitude of both the S and D waves, whereas, the Ar wave will decrease in size [8]. In their quantitative analysis of SVC flow velocities, Byrd and Linden have shown that the ratio of expiratory systolic to diastolic flow velocity in the SVC was high in subjects with cardiac tamponade compared with in healthy individuals and patients with constrictive pericarditis [9]. In patients with chronic pulmonary problems, the expiratory disappearance of the D wave or both S and D waves have been associated with the diagnosis of the chronic obstructive pulmonary disease (COPD) or the presence of combined obstructive and restrictive ventilatory disorders [10].

Little is known about the echocardiographically measured SVC dimension(s). However, in their five normal subjects, Gindea et al. have proved it to be 10 ± 3 mm [11], which is very similar to our findings. SVC dilation has been shown to correlate with that of the IVC as a marker of venous congestion as in patients with congestive heart failure [12]. Ghio and colleagues have also shown that in patients with congestive heart failure, SVC flow velocities can help differentiate those with normal RV hemodynamics from subjects with compensated RV dysfunction and patients with RV failure associated with raised RA pressure [13]. Analysis of respiratory diameter variation of SVC could be helpful to assess fluid challenge in patients with acute circulatory failure. In addition, significant diminution of the SVC – S and Ar waves have been shown to be the most sensitive parameters of blood volume depletion [14]. Furthermore, SVC visualization could help detect the presence of masses, thrombi and device-related vegetations since infection and thrombosis have become the most common complication of longstanding central venous catheters and implantable cardiac devices [15].

### 4.1. Clinical implication

Superior vena cava (SVC) visualization has been hard to do through the classic transthoracic windows for the past several decades. The main

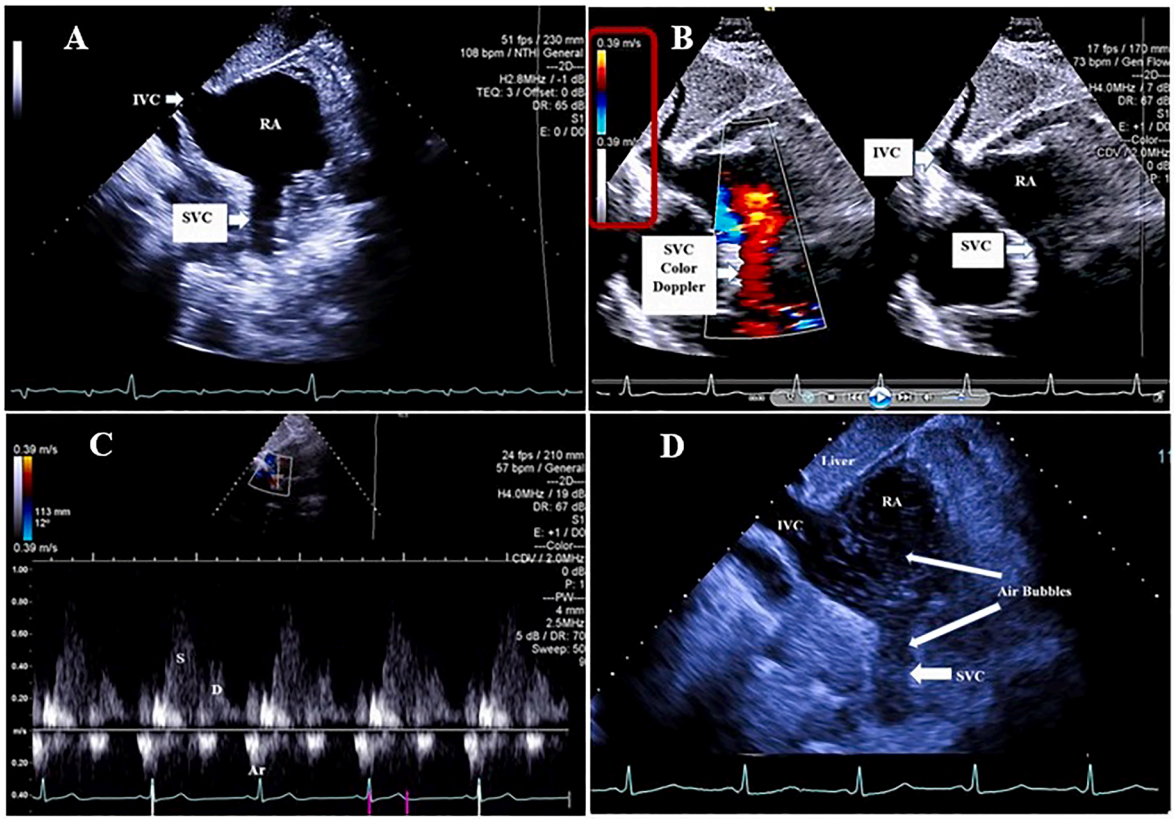


**Fig. 4.** Modified subcostal view. **A)** Two dimensional modified subcostal view for demonstration of proximal SVC. **B)** SVC Color Doppler flow from modified subcostal view (red in color; flow towards the probe). Simultaneous 2D and Colour Doppler Images. **C)** SVC Pulse Wave Doppler flow from modified subcostal view. **D)** Agitated saline injection through peripheral arm vein that filled SVC and partially filled RA to verify SVC course. IVC, inferior vena cava; RA, right atrium; SVC, superior vena cava; S, systolic forward flow; D, diastolic forward flow; Ar, atrial flow reversal. (For interpretation of the references to color in this figure legend, the reader is referred to the web version of this article.)

**Table 1**
Characteristics of the 70 normal participants, including 35 males and 35 females.

| Parameters | Range | Mean ± SD |
|---|---|---|
| Age (years) | 24–45 | 34.9 ± 5.3 |
| Weight (kg) | 46–77 | 61.1 ± 10.3 |
| Height (cm) | 158–178 | 167.6 ± 4.7 |
| Body mass index (kg/m$^2$) | 15.7–27.2 | 21.8 ± 3.6 |

**Table 2**
Superior vena cava dimensions of 70 normal subjects obtained at the end of both cardiac and respiratory cycles.

| Timing | 2DE view | End held expiration | | End held inspiration | |
|---|---|---|---|---|---|
| | | Range (mm) | Mean ± SD (mm) | Range (mm) | Mean ± SD (mm) |
| **End systole** | MSCV | 8–14 | 11 ± 2 | 8–14 | 11 ± 2 |
| | MA5CV | 7–14 | 10 ± 2 | 7–11 | 9 ± 1 |
| | MSAVGV | 8–13 | 10 ± 2 | 8–13 | 10 ± 2 |
| **End diastole** | MSCV | 4–7 | 6 ± 1 | 4–8 | 6 ± 1 |
| | MA5CV | 4–7 | 6 ± 1 | 3–7 | 5 ± 1 |
| | MSAVGV | 3–7 | 5 ± 1 | 3–7 | 5 ± 1 |

**Abbreviations:** MSCV, Modified Subcostal View; MA5CV, Modified Apical 5-Chamber View; MSAVGV, Modified Parasternal Short Axis View of Great Vessels.

**Table 3**
Peak velocities of superior vena cava; S, D and Ar waves obtained at the end-held expiration in 70 normal subjects by the three different proximal SVC visualization road maps.

| View | S-wave | | D-wave | | Ar | |
|---|---|---|---|---|---|---|
| | Range (m/sec) | Mean ± SD (m/sec) | Range (m/sec) | Mean ± SD (m/sec) | Range (m/sec) | Mean ± SD (m/sec) |
| **MSCV** | 0.4–0.7 | 0.5 ± 0.1 | 0.3–0.4 | 0.4 ± 0.0 | 0.2–0.4 | 0.3 ± 0.0 |
| **MA5CV** | 0.4–0.6 | 0.5 ± 0.0 | 0.3–0.4 | 0.4 ± 0.0 | 0.2–0.4 | 0.3 ± 0.0 |
| **MSAVGV** | 0.5–0.7 | 0.6 ± 0.0 | 0.3–0.5 | 0.4 ± 0.1 | 0.2–0.4 | 0.3 ± 0.0 |

**Abbreviations:** MSCV, Modified Subcostal View; MA5CV, Modified Apical 5-Chamber View; MSAVGV, Modified Parasternal Short Axis View of Great Vessels.

accessible sites have been supraclavicular and suprasternal regions with the former being the most popular. Transesophageal echocardiography (TEE) has also been used to see the SVC. However, it is both invasive and expensive and it is not available everywhere.

Transthoracic echocardiography (TTE) is a simple, low-risk procedure and easily available in any hospital. If SVC visualization becomes a routine part of any daily echocardiographic procedure, it would help the implantation and/or extraction of central lines and cardiovascular implantable devices and assist the detection of SVC occlusion and its other pathologies and help early diagnosis and appropriate therapeutic decision making.

**Table 4**
Intraclass correlation coefficient for assessing the reproducibility of the study data.

| Timing | 2DE view | End held expiration | | | End held inspiration | | |
|---|---|---|---|---|---|---|---|
| | | ICC | 95 %CI | P value (ICC = 0) | ICC | 95 % CI | P value (ICC = 0) |
| **End systole** | MSCV | 0.97 | 0.93–0.98 | <0.001 | 0.99 | 0.98–0.99 | <0.001 |
| | MA5CV | 0.93 | 0.87 – 0.97 | <0.001 | 0.98 | 0.97 – 0.99 | <0.001 |
| | MSAVGV | 0.94 | 0.91 –0.97 | <0.001 | 0.95 | 0.89 – 0.97 | <0.001 |
| **End diastole** | MSCV | 0.89 | 0.75–0.94 | <0.001 | 0.98 | 0.96 – 0.99 | <0.001 |
| | MA5CV | 0.97 | 0.93 – 0.98 | <0.001 | 0.97 | 0.96–0.98 | <0.001 |
| | MSAVGV | 0.96 | 0.93–0.98 | <0.001 | 0.95 | 0.93–0.98 | <0.001 |

**Abbreviations:** MSCV, Modified Subcostal View; MA5CV, Modified Apical 5-Chamber View; MSAVGV, Modified Parasternal Short Axis View of Great Vessels; ICC, Intra Class Correlation; CI, Confidence Interval.

**Table 5**
Intraclass correlation coefficient for assessing the reproducibility of the study data.

| View | S-wave | | | D-wave | | | Ar | | |
|---|---|---|---|---|---|---|---|---|---|
| | ICC | 95% CI | P value (ICC = 0) | ICC | 95% CI | P value (ICC = 0) | ICC | 95% CI | P value (ICC = 0) |
| **MSCV** | **0.99** | **0.97 – 0.99** | **<0.001** | **0.88** | **0.76–0.94** | **<0.001** | **0.98** | **0.96–0.99** | **<0.001** |
| **MA5CV** | **0.98** | **0.97–0.99** | **<0.001** | **0.96** | **0.92 –0.99** | **<0.001** | **0.95** | **0.92–0.97** | **<0.001** |
| **MSAVGV** | **0.92** | **0.84–0.96** | **<0.001** | **0.90** | **0.86 – 0.97** | **<0.001** | **0.91** | **0.88–0.94** | **<0.001** |

**Abbreviations:** MSCV, Modified Subcostal View; MA5CV, Modified Apical 5-Chamber View; MSAVGV, Modified Parasternal Short Axis View of Great Vessels; ICC, Intra Class Correlation; CI, Confidence Interval.

What actually is missing in the literature is a simple practical and technical description of "How to visualize the SVC by TTE". Thus we have tried to overcome this issue by description of the fine technical aspects of SVC visualization through the three conventional transthoracic windows.

### *4.2. Study limitations*

Although transthoracic visualization of SVC could be a good initial non-invasive diagnostic imaging of choice, it has its own problems since the presence of a suitable echocardiographic window is mandatory for its successful performance.

Therefore, two main limitations should be considered when interpreting our study results. First, the relatively far depth of the SVC from the selected windows could have made the measurements somewhat difficult, although the maximum SVC depth in our study was about 12–15 cm. Second, to optimize the flow velocity measurements and overcome the problems associated with Doppler angle θ adjustments, by tilting the probe we have tried to optimize the image, get a clear cut vascular flow within the SVC and, keep the Doppler angle θ within an acceptable range, i.e. $\leq$ 30 degrees and choosing the most appropriate point to place the sample volume. The proximity of flow velocity values obtained from these 3 different windows (Table 3), could partly represent this effort.

Another issue is that the study included only young healthy adults since the aim of the study was to get a series of values in an acceptable number of totally normal subjects. Thus, older people were excluded and the results are not applicable to them. Of course, other studies in appropriately selected older people could help solve this problem as well.

One last limitation of this study is that the measurements of proximal SVC diameter have not been validated by other methods. However, SVC measurements by CT and MRI are truly scanty in the literature.

Using ECG-gated CT-angiography, Lin et al [16] have demonstrated that the SVC is often irregular in shape on cross-sectional images. They have suggested a normal range for the major axis (1.5–2.8 cm) and minor axis (1–2.4 cm). Mahlon and Yong [17] have shown the mean length of the SVC to be 7.1 $\pm$ 1.4 cm, and its maximum diameter in adults to be 2.1 $\pm$ 0.7 cm by SVC CT-angiography.

In addition, although SVC-MR venography has been reported for a variety of SVC problems, no data regarding its dimensions could be found in the literature [18,19].

## 5. Conclusion

The study has provided a detailed description of proximal SVC visualization technique through three different transthoracic windows and has furnished sets of values for its dimensions, their respiratory variations as well as its Doppler signal parameters. Therefore, the question of how to visualize the proximal SVC from true transthoracic windows has been properly answered and as such has opened a semi closed SVC-related research window to the interested investigators.

## Funding

This research did not receive any specific grant from funding agencies in the public, commercial, or not-for-profit sectors.

## 7. Availability of data and materials

The data and materials used in this study are available from the corresponding author on reasonable request.

## 8. Statement of authorship

All the authors take responsibility for all aspects of the reliability and freedom from bias of the data presented and their discussed interpretation.

## Declaration of Competing Interest

The authors declare that they have no known competing financial interests or personal relationships that could have appeared to influence the work reported in this paper.

## Acknowledgements

We thank Hossein Sharifkazemi for his invaluable assistance in condensing and collating visualizations for this article.

## Appendix A. Supplementary material

Supplementary data to this article can be found online at https://doi.org/10.1016/j.ijcha.2022.101004.

## References


[1] H. Gray, Anatomy of human body, twenty nineth ed., Lea & Febiger, Philadelphia, 1973.
[2] C. Mitchell, P.S. Rahko, L.A. Blauwet, B. Canaday, J.A. Finstuen, M.C. Foster, et al., Guidelines for Performing a Comprehensive Transthoracic Echocardiographic Examination in Adults: Recommendations from the American Society of Echocardiography, J. Am. Soc. Echocardiogr. 32 (1) (2019) 1–64.
[3] K. Lata, R. Janardhanan, A rare case of SVC syndrome: Accurate diagnosis by multi-modality imaging, J. Ind. Coll. Cardiol. 4 (2014) 119–121.
[4] C.A. Sivaram, P. Craven, K. Chandrasekaran, Transesophageal echocardiography during removal of central venous catheter associated with thrombus in superior vena cava, Am. J. Card. Imaging 10 (4) (1996) 266–269.
[5] S.J. Yakish, A. Narula, R. Foley, A. Kohut, S. Kutalek, Superior vena cava echocardiography as a screening tool to predict cardiovascular implantable electronic device lead fibrosis, J Cardiovasc Ultrasound 23 (1) (2015) 27–31.
[6] M. Nishino, J. Tanouchi, T. Ito, K. Tanaka, T. Aoyama, M. Kitamura, et al., Echographic detection of latent severe thrombotic stenosis of the superior vena cava and innominate vein in patients with a pacemaker: integrated diagnosis using sonography, pulse Doppler, and color flow, Pacing Clin. Electrophysiol. 20 (4 Pt 1) (1997) 946–952.
[7] D.J. Callans, J.F. Ren, D. Schwartzman, C.D. Gottlieb, F.A. Chaudhry, F. E. Marchlinski, Narrowing of the superior vena cava-right atrium junction during radiofrequency catheter ablation for inappropriate sinus tachycardia: analysis with intracardiac echocardiography, J. Am. Coll. Cardiol. 33 (6) (1999) 1667–1670.
[8] N. Nanda, Doppler echocardiography, Igaku-Shoin, Tokyo, 1985.
[9] B.F. Byrd, R.W. Linden, Superior vena cava Doppler flow velocity patterns in pericardial disease, Am. J. Cardiol. 65 (22) (1990) 1464–1470.
[10] S. Kobayashi, S. Izumi, H. Toda, T. Ohta, H. Ochi, Y. Matsuno, et al., Venous return disturbances in chronic pulmonary disease: a study using pulsed Doppler echocardiography, J. Cardiol. 21 (4) (1991) 1009–1015.
[11] A.J. Gindea, J. Slater, I. Kronzon, Doppler echocardiographic flow velocity measurements in the superior vena cava during the Valsalva maneuver in normal subjects, Am. J. Cardiol. 65 (20) (1990) 1387–1391.
[12] M.B.A. Shala, I.A. D'cruz, C. Johns, J. Kaiser, R. Clark, Echocardiography of the Inferior Vena Cava, Superior Vena Cava, and Coronary Sinus in Right Heart Failure, Echocardiography 15 (8) (1998) 787–794.
[13] S. Ghio, F. Recusani, R. Sebastiani, C. Klersy, C. Raineri, C. Campana, L. Lanzarini, A. Gavazzi, L. Tavazzi, Doppler velocimetry in superior vena cava provides useful information on the right circulatory function in patients with congestive heart failure, Echocardiography 18 (6) (2001) 469–477.
[14] J. Liu, T.S. Cao, L.J. Yuan, Y.Y. Duan, Y.L. Yang, Comparison of tricuspid inflow and superior vena caval Doppler velocities in acute simulated hypovolemia: new non-invasive indices for evaluating right ventricular preload, Cardiovasc Ultrasound 4 (2006) 23.
[15] J.I. Sznajder, F.R. Zveibil, H. Bitterman, P. Weiner, S. Bursztein, Central vein catheterization. Failure and complication rates by three percutaneous approaches, Arch. Intern. Med. 146 (2) (1986) 259–261.
[16] F.Y. Lin, R.B. Devereux, M.J. Roman, J. Meng, V.M. Jow, L. Simprini, et al., The right sided great vessels by cardiac multidetector computed tomography: normative reference values among healthy adults free of cardiopulmonary disease, hypertension, and obesity, Acad. Radiol. 16 (8) (2009) 981–987.
[17] M.A. Mahlon, H.C. Yoon, CT angiography of the superior vena cava: normative values and implications for central venous catheter position, J. Vasc. Interv. Radiol. 18 (9) (2007) 1106–1110.
[18] F. Wolf, C. Plank, D. Beitzke, M. Popovic, C.M. Domenig, M. Weber, et al., Prospective evaluation of high-resolution MRI using gadofosveset for stent-graft planning: comparison with CT angiography in 30 patients, AJR Am. J. Roentgenol. 197 (5) (2011) 1251–1257.
[19] C.M. Plank, F. Wolf, H. Langenberger, M. Weber, D. Beitzke, A. Stadler, M. Schillinger, J. Lammer, C. Loewe, Improved detection of in-stent restenosis by blood pool agent-enhanced, high-resolution, steady-state magnetic resonance angiography, Eur. Radiol. 21 (10) (2011) 2158–2165.